

# Gravity observations on Santorini island (Greece): Historical and recent campaigns

Melissinos PARASKEVAS<sup>1,\*</sup> , Demitris PARADISSIS<sup>1</sup>,  
Konstantinos RAPTAKIS<sup>1</sup> , Paraskevi NOMIKOU<sup>2</sup> ,  
Emilie HOOFT<sup>3</sup> , Konstantina BEJELOU<sup>2</sup> 

<sup>1</sup> Dionysos Satellite Observatory, National Technical University of Athens, Polytechnioupoli Zografou, 15780 Athens, Greece, e-mail: melipara1@yahoo.gr, dempar@central.ntua.gr, corapt@central.ntua.gr

<sup>2</sup> Department of Geology and Geoenvironment, National and Kapodistrian University of Athens, Panepistimioupoli Zografou, 15784 Athens, Greece, e-mail: evinom@geol.uoa.gr, bejelouk@gmail.com

<sup>3</sup> Department of Earth Sciences, University of Oregon, OR 97403, Eugene, USA; e-mail: emilie@uoregon.edu

**Abstract:** Santorini is located in the central part of the Hellenic Volcanic Arc (South Aegean Sea) and is well known for the Late-Bronze-Age “Minoan” eruption that may have been responsible for the decline of the great Minoan civilization on the island of Crete. To use gravity to probe the internal structure of the volcano and to determine whether there are temporal variations in gravity due to near surface changes, we construct two gravity maps. Dionysos Satellite Observatory (DSO) of the National Technical University of Athens (NTUA) carried out terrestrial gravity measurements in December 2012 and in September 2014 at selected locations on Thera, Nea Kameni, Palea Kameni, Therasia, Aspronisi and Christiana islands. Absolute gravity values were calculated using raw gravity data at every station for all datasets. The results were compared with gravity measurements performed in July 1976 by DSO/NTUA and absolute gravity values derived from the Hellenic Military Geographical Service (HMGS) and other sources. Marine gravity data that were collected during the PROTEUS project in November and December 2015 fill between the land gravity datasets. An appropriate Digital Elevation Model (DEM) with topographic and bathymetric data was also produced. Finally, based on the two combined datasets (one for 2012–2014 and one for the 1970s), Free air and complete Bouguer gravity anomaly maps were produced following the appropriate data corrections and reductions. The pattern of complete Bouguer gravity anomaly maps was consistent with seismological results within the caldera. Finally from the comparison of the measurements made at the same place, we found that, within the caldera, the inner process of the volcano is ongoing both before, and after, the unrest period of 2011–2012.

**Key words:** Santorini, gravity, Bouguer, Free Air Anomaly, HMGS

\*corresponding author: e-mail: melipara1@yahoo.gr

## 1. Introduction

Earth’s gravity is a physical force resulting from the gravitational attraction due to the planet’s mass and a centrifugal term due to Earth’s rotation. Geophysicists use gravity to better understand deep structures of the Earth by modelling their density distributions with depth. Gravity variations result from a variety of processes including variations in: elevation, mean density of an area, latitude, and/or the particular time measurements were made. At volcanos, careful analysis of temporal variations in gravity can be used to identify changes in the near-surface volcanic system (e.g. *Battaglia et al., 2008; Williams-Jones et al., 2008; Vajda, 2016*).

Santorini volcanic complex is located in the central part of the Hellenic Volcanic Arc (South Aegean Sea) (Fig. 1), and consists of Thira (Santorini), Palea Kameni, Nea Kameni, Aspronisi, Thirassia and the active submarine volcano of Kolumbo. Santorini is also well known for the Late-Bronze-Age “Minoan” eruption that might have been responsible for the decline of the great Minoan civilization on the island of Crete. The volcano was in a quiet, rest period from 1950 to 2011. In January 2011, Santorini entered a phase of unrest, which lasted until March 2012 (e.g. *Parks et al., 2012; Newman et al., 2012*). Onshore measurements of the gravitational field were carried out after the unrest period in December 2012 (Fig. 1d) and September 2014 (Fig. 1e) as discussed by *Paraskevas et al. (2014; 2019)*. To probe the gravity field prior to the unrest period, Dionysus Satellite Observatory of National Technical University of Athens (DSO/NTUA) obtained a set of measurements for Santorini island, that has existed since 1976 (*Agatzabalodimou and Papazissi, 1984*) (Fig. 1b). Furthermore, a 1969 gravity dataset from *Yokoyama and Bonasia (1978)* (Fig. 1a) and gravity values from the Hellenic Military Geographical Service (HMGS) (Fig. 1c) were integrated with the national gravity network at various times. In addition, offshore gravity data were collected during the PROTEUS project in November and December 2015 (*Hooft et al., 2015*) (Fig. 1f).

The aim of this paper is to make two gravity maps for the Santorini volcanic group (Thira, Thirassia, Palea and Nea Kameni and Aspronisi) that are adjusted to a comparable gravity datum. One map represents the period prior to the Santorini unrest in 2011–2012 and includes data from the 1970s. The second map is for the years following the unrest period and includes data from 2012–2014.

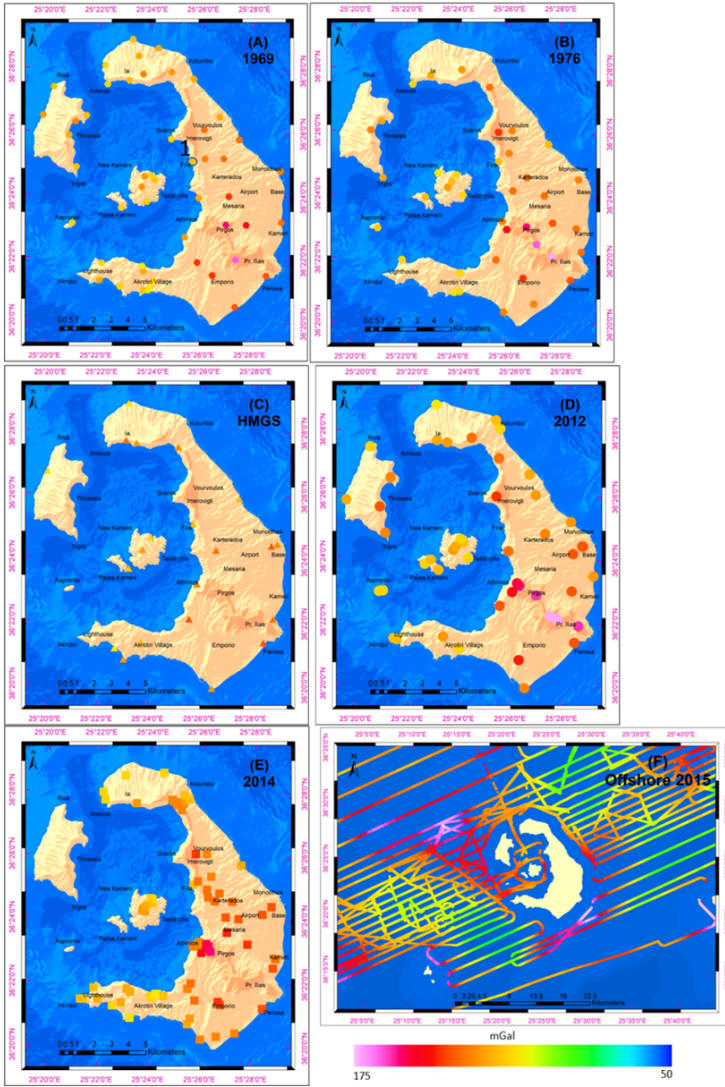


Fig. 1. It shows the spatial distribution of Free Air Anomalies of all datasets overlaying a produced terrain-bathymetry model. (a) 50 station refer to station 1 (Fira) after *Yokohama and Bonasia (1978)*, (b) 41 stations refer to Piraeus port after *Agatza-Balodimou and Papazissi (1984)*, (c) 20 stations graded by HMGS refer to old National Gravity Station, (d) 53 stations refer to HMGS after *Paraskevas et al. (2014; 2019)*, (e) 83 stations refer to HMGS after *Paraskevas et al. (2014; 2019)*, (f) Offshore Gravity measurements refer to HMGS after *Paraskevas et al. (2019)*.

## 2. Data and methods

### A. Coordinate system

The selected coordinate system for this research is WGS84 (G1674 edition). To be compatible with this system, every gravity measurement needs an appropriate transformation from the time of the measurement to the selected coordinate system. The datasets of 1976 and 1969 were picked from maps using Hayford geographic coordinates, while the more recent datasets were measured in the WGS84 geographic system. The accurate position of each station measured in 1976 and 1969 was calculated using a local transformation between the two systems and corrected with descriptions of each station. New geographic coordinates for stations measured in 1976 and 1969 were picked from orthophotos with accuracy better than 2 m.

The gravity datum selected was the unpublished yet Local Hellenic Gravity Datum from HMGS (epoch 2014). Datasets of 1976 and 1969 were shifted to a proper reference station to correspond to the selected gravity datum. Gravity values that refer to the Potsdam gravity datum were transformed to the IGSN71 gravity network subtracting  $14.884 \cdot 10^{-5} \text{ m/s}^2$  (mGal), which is the measured difference between the National Gravity Station in HMGS and IGSN71.

### B. Earth and ocean tides

Earth tides for the dataset of 1969 and benchmarks graded from HGMS were calculated using Longman's Formula (*Longman, 1959*) with estimated accuracy of  $4\text{--}5 \mu\text{Gal}$  as shown by *Yu et al. (2019)*. For gravity datasets with raw gravity measurements (1976, 2012, 2014), Earth and ocean tides were corrected using an unpublished MATLAB code that includes IERS treaties (International Earth Rotation and Reference Systems Service) (*Petit and Luzum, 2010*), precise ephemeris from <https://www.jpl.nasa.gov/> and the ocean model FES2004 (*Lyard et al., 2006*). The functions of the code were described by *Papanikolaou (2012)*.

### C. Onshore gravity datasets

#### I. Gravity survey of 1969

*Yokohama and Bonasia (1978)* carried out a gravity survey at 50 stations

(Fig. 1a). Their results are available at the Bureau Gravimetricque International (*BGI*). These measurements were also included in the HMGS report of 1976. The standard deviation of each measurement was better than 0.060 mGal and all measurements referred to the base station of Santorini island at Fira port, which was included in the old National Gravity Network, with a reported difference from station 1 (Fig. 1a) of 0.127 mGal. For this study, the absolute gravity values refer to the Potsdam base station and were transformed to the IGSN 71 reference network and from there to the selected gravity datum. Reported elevations of each station were measured using barometers and psychrometers, so their accuracy is probably 1–2 metres. New elevations for every measurements were used in this research using the produced 5 metre-DEM (*Paraskevas et al., 2014*).

## *II. Gravity survey of 1976*

In 1976, *Agatza-Balodimou and Papazissi (1984)* from the National Technical University of Athens (NTUA) carried out a series of measurements on Santorini island using La Coste & Romberg G51 and G63 gravimeters (Fig. 1b). Besides that, three Thomson altimeters and one Assman psychrometer were used to obtain altitude information. Detailed descriptions of each benchmark study were used to improve their location and elevation.

This gravity campaign was connected, via Piraeus' port, to two base gravity stations at the NTUA (School of Architecture in Athens and Department of Topography in Zografou) to determine absolute gravity values. The adjusted gravity difference from these stations to the National Gravity Station of HMGS was used to reference all measurements to the same datum.

During data processing, raw measurements were corrected for a reading factor (according to La Coste & Romberg recommendation table) and for the Earth tide effect (*Papanikolaou, 2012*). Finally, a linear approximation model was employed to correct for daily drift in the data. This campaign took place from 19/4/1976 to 2/5/1976 and it was carried out in nine day-loops. Corrected measurements for drift and tide effects were adjusted simultaneously using the least squares adjustment method (*Torge, 1989*) without weights. The resolution of these gravimeters (L & R type G), is 10  $\mu$ Gal and the best achievable accuracy is up to 15  $\mu$ Gal according to *Seigel (1995)*. The resolution of the gravimeter (10  $\mu$ Gal) was added to

the adjustments' standard deviation for each measurement. The derived precision (standard deviation) of the calculated absolute gravity values was 0.012 to 0.071 mGal (Appendix 1).

### *III. Various gravity surveys reported by HMGS*

HMGS carried out repeated gravity measurements in the Santorini area as part of a project that took place in 1966, 1969, and 1975 (Fig. 1c). All these measurements were made using 3 Lacoste & Romberg gravimeters and one Worden gravimeter. The reported standard deviation (SDV) of these observations is between 0.011 and 0.049 mGal and the absolute gravity values are referenced to the old HMGS gravity station. Gravity values were shifted to refer to National Gravity Station of HMGS (2014) by adding the measured difference between old and new National gravity station ( $g_{\text{old National Gravity Station}} - g_{\text{new National Gravity Station}} = 0.084$  mGal).

HMGS established and made repeated measurements at the gravity station near Santorini airport, which was one of the stations of the earliest campaign. This gravity station belongs to the First Order National Gravity Network, which implies that it is very accurate and its results remain stable for years. The most recent measurements for the First Order National Network were made in 2005. For these measurements 3 Lacoste & Romberg gravimeters type G and one type D (resolution 0.001 mGal) were used. According to an unpublished HMGS First Order gravity stations report of 2015 the standard deviation for the Santorini station was 0.010 mGal using 8 independent measurements.

### *IV. Gravity campaign of 2012*

In 2012 gravity measurements were collected using a Scintrex CG5 gravimeter. The observations include 53 stations (Fig. 1d) 36 of which are at known orthometric heights. Furthermore, a GPS Promark 100 receiver was used to measure elevation 3–5 metres around each benchmark.

The campaign took place from 10 to 16/12/2012 and was connected with the National Gravity Station of HMGS through the “El. Venizelos” airport, by repeated measurements with air transport. For every datum location, at least two successive measurements were taken to ensure repeatability. In addition, as it is essential in any precise gravity survey, nearly all stations were revisited several times, either on the same loop to check for drift, or

on a different loop to tie loops together.

Final measurements were adjusted together by the least squares adjustment method (*Torge, 1989*) using as standard deviation of each measurement the recorded SDV of the appropriate gravimeter. The derived standard deviation (precision) of the calculated absolute gravity values was better than 0.016 to 0.037 mGal (Appendix 2).

#### *V. Gravity campaign of 2014*

This campaign aimed to fill gaps in the 2012 measurements and was performed from 23 to 28/9/2014 using the same instrumentation as in the campaign of 2012. The observations include 83 additional stations (Fig. 1e) and the measurements were connected to the National Gravity Station of HGMS through the Piraeus port control point, by repeated measurements with ship transport.

Gravimeter static drift was calculated offline before and after the campaign at the gravity station of DSO/NTUA using 24h measurements. Earth tide effects for each station were calculated offline using the code of *Papanikolaou (2012)*, while all other available corrections were made using the software of the gravimeter (tilt, temperature correction, and seismic filter).

Final measurements were adjusted together by the least squares adjustment method (*Torge, 1989*) using as standard deviation (SDV) of each measurement the recorded SDV of the gravimeter. The derived standard deviation of the calculated absolute gravity values was better than 0.009 to 0.031 mGal (Appendix 3).

#### **D. Offshore gravity measurements**

Marine gravity measurements were collected during the PROTEUS project (*Hooft et al., 2015*) in November and December 2015 using BGM-3 gravimeter (SN S224) on the R/V Marcus Langseth, cruise MGL1521, and are available from <https://www.rvdata.us/> (Fig. 1f). Firstly, ship gravity data were merged with navigation data (date, time, ship's speed, water depth, course, latitude and longitude). The processing procedure also includes a Gaussian 240 second filter, a median filter of 480 seconds, a non-linear filter of 60 seconds, Eötvös Correction and tide correction. Measurements were adjusted to the National Gravity Station of HGMS through the Piraeus

port. Long term static drift was calculated from relative gravity differences at Piraeus port in the beginning and at Heraklion port at the end of the campaign, using absolute gravity values of National gravity network. Calculated long term drift was 0.02 mGal/day. Finally, crossover analysis and adjustment was applied (using the method of *Hsu (1995)*). The derived standard deviation of crossover adjusted values was better than 0.5 mGal.

### E. Digital Terrain Model and seafloor topography

Various data were used to develop a detailed Digital Terrain Model that includes seafloor topography: (i) geometric altitudes from the NTUA network from 56 locations, (ii) a 5-metre DTM graded from the Hellenic Military Geographic Agency (HMGA) generated from combined photogrammetric methods and height measurements, (iii) orthometric and geometric heights at geodetic control points obtained by the HMGA, (iv) height measurements with GPS receivers, (v) 10 m seafloor contours derived from HMGA, (vi) high resolution swath data provided by *Nomikou et al. (2014)*, (vii) the high resolution GDEM of ASTER v2 (*NASA and METI, 2011*), (viii) the recent coastline from HMGA and (ix) Lidar data from *Nomikou et al. (2014)*. A dense Digital Elevation Model (DEM) with pixel size of 5 m was created in the area of interest and a rather rough DEM with pixel size of 100 m in the surrounding areas.

### F. Global Geopotential Model (GGM)

Two GGM were tested in the area of this research: EGM2008 (*Pavlis et al., 2012*) and EIGEN6C4 (*Förste et al., 2014*), until order and degree 2190. These models were tested at 128 measured stations during the 2012–2014 campaigns, comparing measured free air gravity anomalies with calculated ones from GGM at the same point, using MATLAB code after *Papanikolaou (2013)*. Table 1 shows that both GGM fit the measured data very well, compared to other areas at Greece (*Papadopoulos et al., 2019*). EGM2008 performed slightly better and consequently this is the selected GGM.

### G. Reduction scheme

The reduction scheme for final adjusted absolute gravity values (*Gabs*) includes:

Table 1. Comparison of GGMs in 128 gravity stations measured in 2012 and 2014 at Santorini complex.

Statistics	128 gravity stations	
	EGM2008 [mGal]	EIGEN6C4 [mGal]
Min	6.04	26.63
Max	69.08	87.81
Mean	24.86	38.27
SDV	11.34	13.04

- Geographic latitude corrections (Normal gravity): Normal Gravity for all gravity data was calculated to WGS84 ellipsoid using the closed Somigliana’s formula (Somigliana, 1930):

$$G_{mod} = ge * \frac{1 + k \sin^2 \varphi}{\sqrt{1 - e^2 \sin^2 \varphi}}, \quad (1)$$

where  $G_{mod}$  is normal gravity at WGS84 ellipsoid,  $ge = 978032.67714$  mGal,  $k = 0.00193185138639$ ,  $e^2 = 0.00669437999013$ , and  $\varphi$  is the latitude of the station in decimal degrees (Hofmann-Wellenhof and Moritz, 2005).

- Free air reduction: The simply free air gradient was used:

$$\delta g_{FA} = -0.3086 H, \quad (2)$$

where  $H$  is the orthometric height above sea level in metres.

- Bouguer spherical cap: The Bouguer spherical cap models a simple mass from the ellipsoid to the station height. A simple Bouguer reduction was calculated using equation 3 (Hildenbrand et al., 2002):

$$\delta g_{BC} = 2\pi G\rho(\mu h - \lambda R), \quad (3)$$

where  $G = 6.674 \times 10^{-11} \text{ Nm}^2/\text{kg}^2$  is the universal gravitational constant,  $\rho$  is the mean density of the rock material of the plate (here  $2670 \text{ kg/m}^3$ ),  $\mu$  and  $\lambda$  are dimensionless coefficients (LaFehr, 1991),  $h$  is the height of the gravity station above the GRS80 reference ellipsoid (km), and  $R$  is the combined height of the gravity station and average radius of Earth (km).

- *Terrain Correction (TC)*: Terrain correction was calculated using the algorithm proposed by *Nagy (1966)* and *Kane (1962)*. To calculate corrections, the produced DTM5 was ‘sampled’ to a grid mesh centred on the station to be calculated. The correction was calculated based on near zone, intermediate zone, and far zone contributions. In the near zone, 0 to 5 m from the station, the algorithm sums the effects of four sloping triangular sections, measured around the station (the surface between the station and the elevation at each diagonal corner of the pixel of produced DTM was used). The calculation was done using Eq. (4) (*Nagy, 1966*):

$$g = G\rho\varphi \left( R - \sqrt{R^2 + H^2} + \frac{H^2}{\sqrt{R^2 + H^2}} \right), \quad (4)$$

where  $g$  is the gravitational attraction,  $\rho$  the terrain density (here 2.67 g/cm<sup>3</sup>),  $\varphi$  the horizontal angle of the triangular section,  $G$  the gravitational constant,  $H$  the difference between the station elevation and the average elevation of the diagonal corner, and  $R$  the specific distance (here 5 m).

In the intermediate zone (5 to 40m), the terrain effect is calculated for each point using the flat-topped square prism approach of *Nagy (1966)* (Eq. (6)). The terrain height is measured on a regular grid (equal spacing) with a total of  $N \times M$  points. Then the terrain correction can be computed by summing up these  $N \times M$  prisms using Eq. (5):

$$g = G\rho \left| \int_{z_1}^{z_2} \int_{y_1}^{y_2} \int_{x_1}^{x_2} x \ln(y+r) + y \ln(x+r) - z \sin^{-1} \left( \frac{z^2 + y^2 + yr}{(y+r)\sqrt{y^2 + z^2}} \right) \right|, \quad (5)$$

where  $g$  is the vertical component of the attraction,  $\rho$  the density (here 2.67 g/cm<sup>3</sup>),  $G$  the gravitational constant, and  $r$  the distance between a unit mass and the station.

In the far zone (40 m to 200 km), the terrain effect is derived based on the approximation of an annular ring segment to a square prism, as described by *Kane (1962)*. The gravitational attraction is calculated by Eq. (6) (*Kane, 1962*):

$$g = 2G\rho A^2 \frac{\left( R_2 - R_1 \sqrt{R_1^2 + H^2} - \sqrt{R_2^2 + H^2} \right)}{\left( R_2^2 - R_1^2 \right)}, \quad (6)$$

where  $g$  is the gravitational attraction,  $\rho$  the terrain density (here  $2.67 \text{ g/cm}^3$ ),  $A$  the length of the horizontal side of the prism,  $R_1$  the radius of the inner circle of the annular ring,  $R_2$  the radius of the outer circle of the annular ring, and  $H$  the height of the annular ring or prism (we neglect the error at calculations using Eq. (6) from the Earth curvature because it is under standard error of our measurements).

## H. Gravity anomalies

According to the above reduction schema, gravity anomalies can be calculated by the equations:

$$FAA = Gabs - Gmod - \delta gFA, \quad (7)$$

$$SBG = FAA - \delta gBC, \quad (8)$$

$$CBG = SBG + TC, \quad (9)$$

$FAA$  stands for free air anomaly,  $SBG$  represents simple Bouguer gravity anomaly and  $CBG$  is complete Bouguer gravity anomaly.

## I. Interpolation

To generate gravity anomaly maps for geological interpretation, gravity anomalies need to be expressed on a regular grid. However, gravity measurements are not homogeneously distributed. According to *Eckstein (1989)*, due to the fact that the effectiveness of a particular interpolation method depends on the distribution of the observations and field gradients, no gridding algorithm should be considered “perfect”. Nevertheless, some interpolation approaches are more suitable than others. Using a “trial and error” approach, Empirical Bayesian Kriging was selected, which creates a spectrum of semi-variograms, contrary to other Kriging methods that assume that the estimated semi-variogram is the true one for the observed data.

The selected gridding method minimizes the standard prediction error of the actual data as well as the difference in predicted and measured values at 10 carefully selected independent benchmark studies, which were not used in the interpolation. Parameters for the selected interpolation method are presented in Table 2.

Table 2. Parameters and statistics of the selected interpolation method.

Gridding method	Subset size (values)	Semi-variogram type	Neighbourhood type	Neighbours (values)	Sector	Radius (metres)	Average standard error (mGal)	Max error in independent measurements (mGal)
Empirical Bayesian kriging	60	Power	Standard circular	10	4	2500	2.1154	0.448

### 3. Results

#### A. Maps and statistics

To achieve sufficient coverage, it was necessary to adjust the 1969, 1976, and HMGS gravity datasets together to produce the “older” gravity map. Additionally, the 2012 and 2014 datasets were adjusted together to produce the newer gravity map. To add offshore coverage, the latter two datasets were combined with the marine gravity survey of 2015.

Figures 2 and 3 and Table 3 show the final results for the two datasets. Results of both datasets are very similar; small differences are due to the distribution of measurements. Regional maxima, present in both datasets, are found at Athinios, Fira and Profitis Ilias, where the geologic formations seem to be more dense, as they represent pre-volcanic units (*Druitt, 2014*). Regional minima, also present in both datasets, were observed southwest of Oia and Akrotiri Village and coincide with the Kolumbo fault zones and Akrotiri earlier geological formations (*Druitt, 2014*), respectively (Fig. 4).

Table 3. Statistics of free air and complete Bouguer gravity anomalies for each dataset.

	FAA_70s	FAA_2014	CBG_70s	CBG_2014
min	70.552	70.432	98.38	97.724
max	169.203	171.652	143.144	143.113
mean	104.46	104.558	120.357	120.446
stdv	16.307	16.532	9.008	8.996

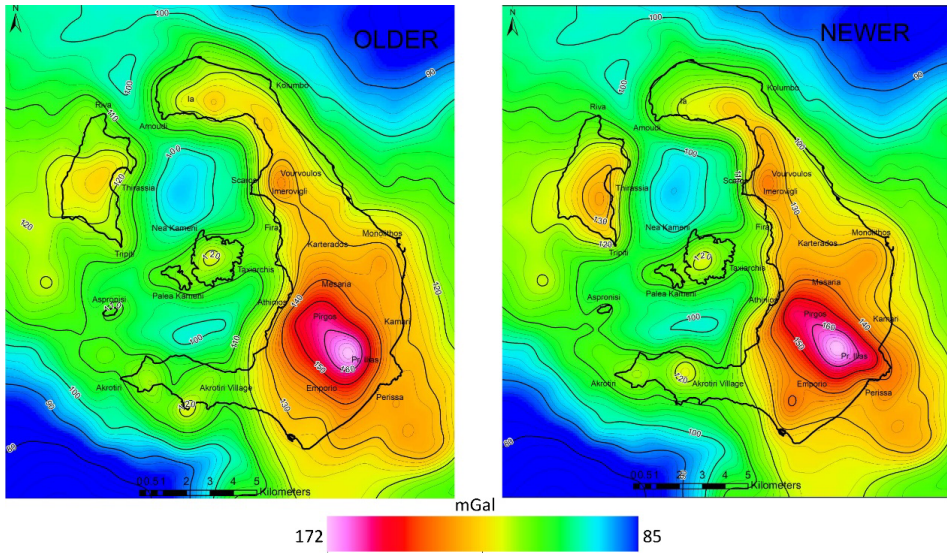


Fig. 2. Free air gravity anomalies in the area of Santorini, (a) using gravity measurements from 1966 to 1976, (b) using the datasets of 2012 and 2014. Contour interval is 2 mGal. Empirical Bayesian kriging was used for interpolation.

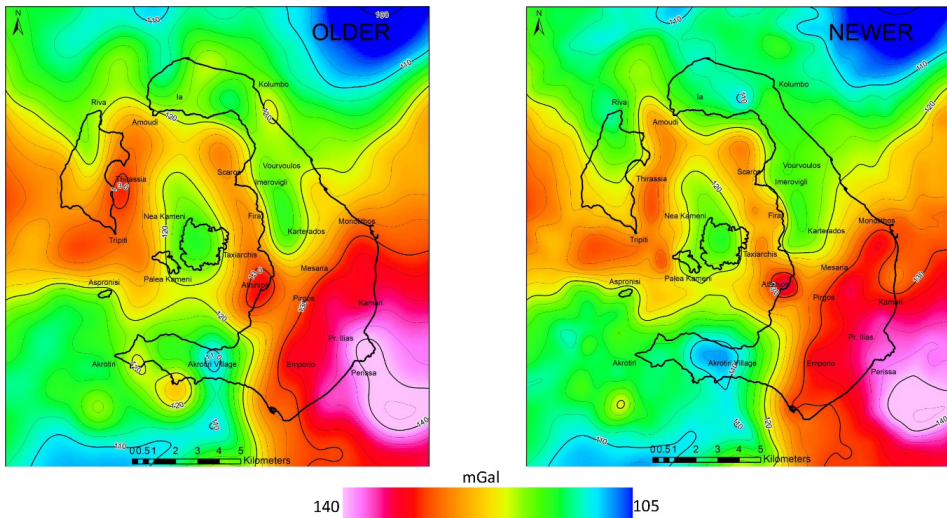


Fig. 3. Complete Bouguer gravity anomalies at the area of Santorini (a) using gravity values from 1966 to 1976, (b) using the datasets of 2012 and 2014. Contour interval is 2 mGal. Empirical Bayesian kriging was used for interpolation.

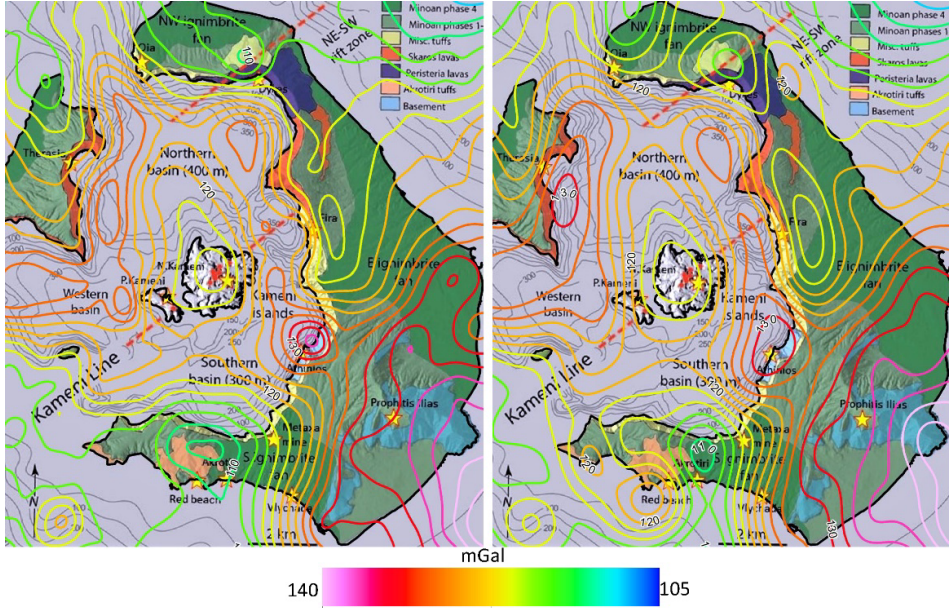


Fig. 4. Complete Bouguer gravity anomalies at the area of Santorini over simplified geologic map of the Santorini volcanic complex (*Druitt, 2014*), (a) using the datasets of 2012 and 2014, (b) using gravity values from 1966 to 1976. Contour interval is 2 mGal.

## B. Analysis

The Complete Bouguer Gravity Anomaly maps for both datasets reveal a nearly elliptical zone at the centre of the caldera that includes the islands of Palea and Nea Kameni and the calculated Mogi-point inflation source for the 2011–2012 unrest period (e.g., *Parks et al., 2012; Newman et al., 2012*). These results are also consistent with the P-wave seismic velocity structure of Santorini that reveals a low-velocity anomaly in the upper 3 km, with a diameter of  $3 \pm 0.5$  km, which is confined beneath the north-central portion of the caldera (*Hooft et al., 2019*).

A quantitative analysis for temporal gravity changes was performed by comparing values at exactly the same point for both datasets (Fig. 5). Table 4 shows that there are significant differences in absolute gravity values around the centre of the caldera. In contrast, for the rest of the island the differences are near the standard deviation of each station. This implies that

the inner processes of the volcano are still active. More detailed analysis will be the main objective of another paper.

Table 4. Gravity variation with time at same benchmarks measured at different epochs.

station	latitude	longitude	elevation	dyear	dg	SDV	annual dg
units	dec degrees	dec degrees	metres		mGal	mGal	$\mu$ Gal/year
Nea Kameni Port	36.4110	25.4003	1.465	2014–1976	0.256	0.031	6.74
Nea Kameni middle	36.4104	25.4012	2.010	2014–1975	0.246	0.042	6.30
Centre of Nea Kameni	36.4045	25.3949	126.737	2012–1976	0.385	0.027	10.70
Taxiarchis (N. Kameni)	36.4004	25.4049	2.962	2012–1976	0.290	0.025	8.06
Palea Kameni	36.3990	25.3805	1.021	2012–1976	0.277	0.027	7.69
Athinios	36.3868	25.4308	1.596	2014–1976	0.076	0.015	2.01
Aspronisi	36.3825	25.3490	3.200	2012–1976	0.020	0.068	0.54
base	36.4073	25.4786	34.610	2012–2004	0.015	0.009	1.84
Emporeio Sq	36.3571	25.4447	76.548	2014–1976	−0.014	0.037	−0.36
Vourvoulos	36.4346	25.4362	123.537	2014–1976	0.008	0.026	0.20
Perissa	36.3566	25.4744	4.400	2012–1975	0.037	0.025	1.01
South West of Oia	36.4607	25.3900	155.730	2012–1975	0.062	0.017	1.68
Fira	36.4183	25.4277	1.140	2014–1968	0.062	0.024	1.34
airport	36.4031	25.4727	52.100	2014–2012	−0.006	0.014	−2.85
Church Athinios	36.3862	25.4381	299.101	2014–2012	0.007	0.019	3.65
lighthouse	36.3576	25.3571	99.360	2012–1975	0.009	0.044	0.24

## 4. Conclusions

To probe the internal structure of Santorini volcano and to determine whether there are temporal variations in gravity due to near surface changes, we construct two gravity maps. We carefully applied data correction and gridding to several historic gravity datasets to produce two gravity anomaly maps that correspond to the years before and after the 2011–2012 volcanic unrest episode at the volcano (the 1970s and 2012–2014, respectively). Through a comparative study, there are not significant qualitative differ-

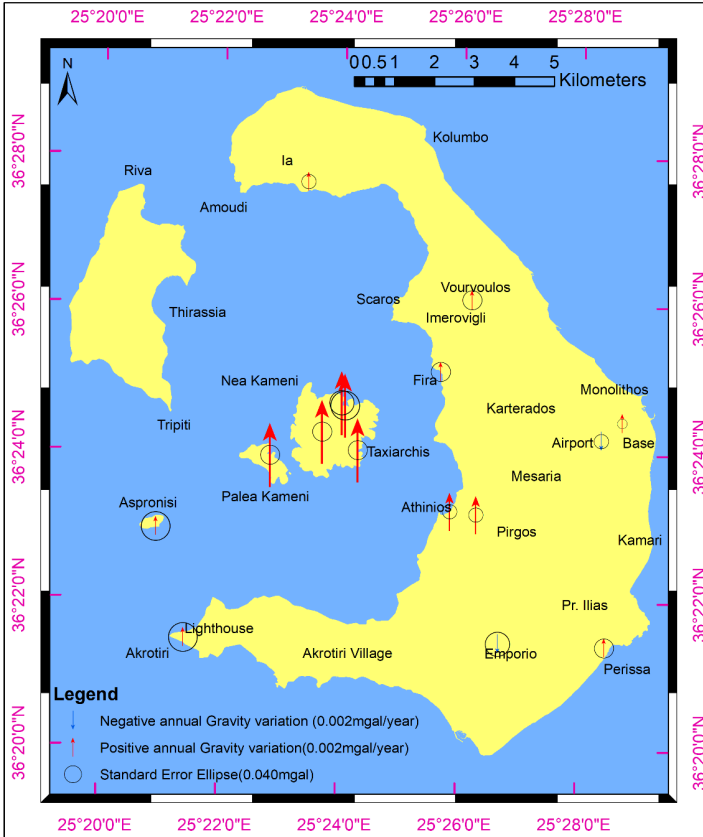


Fig. 5. Annual gravity variation with time at same benchmarks measured at different epochs.

ences between the two maps. An almost elliptical gravity minimum near the centre of the caldera is in good agreement with the seismic low velocity structure of *Hooft et al. (2019)*. Regional maxima were observed in both maps at Athinios, Fira and Pr. Ilias, where the rock units are more dense. Regional minima in both datasets are located southwest of Oia and at Akrotiri Village, coinciding with the Kolumbo and Akrotiri fault zones, respectively. Significant differences in the complete Bouguer gravity anomalies between the two maps were only found within the caldera, indicating temporal changes in density of the upper crust that suggest that the inner process of the volcano is still active.

**Acknowledgements.** The authors are indebted to the Hellenic Military Geographical Service for the data and instrumentation that they provided. The marine gravity data collection was supported by the US National Science Foundation under grant number OCE-1459794 to the University of Oregon.

## References

- Agatza-Balodimou A. M., Papazissi K., 1984: The gravity field of Santorini, *Techn. Chron. – A, Greece*, **4**, 4, 5–17 (in Greek with with English summary).
- Battaglia M., Gottsmann J., Carbone D., Fernández J., 2008: 4D volcano gravimetry. *Geophysics*, **73**, 6, WA3–WA18, doi: 10.1190/1.2977792.
- Bureau Gravimétrique International (BGI): Gravity measurements published at <http://bgi.obs-mip.fr>, doi: 10.18168/BGI.
- Druitt T. H., 2014: New insights into the initiation and venting of the Bronze-Age eruption of Santorini (Greece), from component analysis. *Bull. Volcanol.*, **76**, 794, doi: 10.1007/s00445-014-0794-x.
- Eckstein B. A., 1989: Evaluation of spline and weighted average interpolation algorithms. *Comput. Geosci.*, **15**, 1, 79–94, doi: 10.1016/0098-3004(89)90056-3.
- Förste Ch., Bruinsma S. L., Abrikosov O., Lemoine J.-M., Schaller T., Götze H.-J., Ebbing J., Marty J. C., Flechtner F., Balmino G., Biancale R., 2014: EIGEN-6C4 – The latest combined global gravity field model including GOCE data up to degree and order 2190 of GFZ Potsdam and GRGS Toulouse. In: *Proceedings of 5th International GOCE User Workshop, Paris 25 – 28 Nov. 2014*.
- Hildenbrand T. G., Briesacher A., Flanagan G., Hinze W. J., Hittelman A. M., Keller G. R., Kucks R. P., Plouff D., Roest W., Seeley J., Smith D. A., Webring M., 2002: Rationale and operational plan to upgrade the U.S. gravity database. U.S. Geological Survey Open-File Report, 2002-463, 12 p., doi: 10.3133/ofr02463.
- Hofmann-Wellenhof B., Moritz H., 2005: *Physical Geodesy*. Springer-Verlag Wien, 403 p., doi: 10.1007/b139113.
- Hooft E. E. E., Toomey D. Nomikou P., 2015: PROTEUS: Plumbing reservoirs of the Earth under Santorini. MGL1521 Cruise report 2015, website: <https://pages.uoregon.edu/emilie/PROTEUS/>.
- Hooft E. E. E., Heath B. A., Toomey D. R., Paulatto M., Papazachos C. B., Nomikou P., Morgan J. V., Warner M. R., 2019: Seismic imaging of Santorini: Subsurface constraints on caldera collapse and present-day magma recharge. *Earth Planet. Sci. Lett.*, **514**, 48–61, doi: 10.1016/j.epsl.2019.02.033.
- Hsu S.-K., 1995: XCORR: A cross-over technique to adjust track data. *Comput. Geosci.*, **21**, 2, 259–271, doi: 10.1016/0098-3004(94)00070-B.
- Kane M. F., 1962: A comprehensive system of terrain corrections using a digital computer. *Geophysics*, **27**, 4, 455–462, doi: 10.1190/1.1439044.
- LaFehr T. R., 1991: An exact solution for the gravity curvature (Bullard B) correction. *Geophysics*, **56**, 8, 1179–1184, doi: 10.1190/1.1443138.
- Lyard F., Lefevre F., Letellier T., Francis O., 2006: Modelling the global ocean tides: modern insights from FES2004. *Ocean Dyn.*, **56**, 5–6, 394–415, doi: 10.1007/s10236-00

6-0086-x.

- Longman I. M., 1959: Formulas for computing the tidal accelerations due to the moon and the sun. *J. Geophys. Res.*, **64**, 12, 2351–2355, doi: 10.1029/JZ064i012p02351.
- Nagy D., 1966: The gravitational attraction of a right rectangular prism. *Geophysics*, **31**, 2, 362–371, doi: 10.1190/1.1439779.
- NASA and METI, 2011: ASTER Global Digital Elevation Model (GDEM) v2 data is a product of NASA and METI, released at October 17, 2011, pixel size 30 meters.
- Newman A. V., Stiros S., Feng L., Psimoulis P., Moschas F., Saltogianni V., Jiang Y., Papazachos C., Panagiotopoulos G., Karagianni E., Vamvakaris D., 2012: Recent geodetic unrest at Santorini Caldera, Greece. *Geophys. Res. Lett.*, **39**, 6, L06309, doi: 10.1029/2012GL051286.
- Nomikou P., Parks M. M., Papanikolaou D., Pyle D. M., Mather T. A., Carey S., Watts A. B., Paulatto M., Kalnins M. L., Livanos I., Bejelou K., Simou E., Perros I., 2014: The emergence and growth of a submarine volcano: The Kameni islands, Santorini (Greece). *GeoResJ*, **1-2**, 8–18, doi: 10.1016/j.grj.2014.02.002.
- Papadopoulos N., Paraskevas M., Katsafados I., Nikolaidis G., 2019: Calculating a geoid model for Greece using gravity and GPS observations. Conference JISDM 2019, May 2019, doi: 10.13140/RG.2.2.22623.71841/1.
- Papanikolaou T. D., 2012: Dynamic modelling of satellite orbits in the frame of contemporary satellite geodesy missions. Ph.D. Dissertation, Aristotle University of Thessaloniki, Greece (in Greek).
- Papanikolaou T. D., 2013: Development of GRAVsynth software for spherical harmonic synthesis. User guide, Department of Gravimetry, Hellenic Military Geographical Service, Athens, Greece (in Greek).
- Paraskevas M., Paradissis D., Kolovos I., Nomikou P., Papanikolaou D., Raptakis C., 2014: Tectonic structure of Santorini volcanic field based on terrestrial gravity measurements (1976–2012). In: 1st International Geo-Cultural Symposium Kaldera, 6–8 June 2014, Santorini, Greece, [http://www.mesonisos.gr/images/ABSTRACT\\_VOLUME.pdf](http://www.mesonisos.gr/images/ABSTRACT_VOLUME.pdf).
- Paraskevas M., Paradissis D., Raptakis C., Nomikou P., Hooft E. E., Papanikolaou D., 2019: Geodetic and geophysical approach of the gravitational field in Santorini Volcanic Group, Conference JISDM 2019, Athens, Greece, May 2019, doi: 10.13140/RG.2.2.15196.03209.
- Parks M. M., Biggs J., England P., Mather T. A., Nomikou P., Palamartchouk K., Papanikolaou X., Paradissis D., Parsons B., Pyle D. M., Raptakis C., Zacharis V., 2012: Evolution of Santorini Volcano dominated by episodic and rapid fluxes of melt from depth. *Nat. Geosci.*, **5**, 749–754, doi: 10.1038/ngeo1562.
- Pavlis N. K., Holmes S. A., Kenyon S. C., Factor J. K., 2012: The development and evaluation of the Earth Gravitational Model 2008 (EGM2008). *J. Geophys. Res.*, **117**, B4, B04406, doi: 10.1029/2011JB008916.
- Petit G., Luzum B., 2010: IERS Conventions (2010), IERS Technical Note No. 36. Verlag des Bundesamts für Kartographie und Geodäsie, Frankfurt am Main.
- Seigel H. O., 1995: A guide to high precision land gravimeter surveys. Scintrex Limited, Canada, 132 p.

- Somigliana C., 1930: Sul campo gravitazionale esterno del geoide ellissoidico. *Atti della Accademia nazionale dei Lincei Rendiconti, Classe di scienze fisiche, matematiche e naturali. Geofisica*, 237–243.
- Torge W., 1989: *Gravimetry*. de Gruyter, Berlin–New York 1989, p. 327–328.
- Vajda P., 2016: Recent Developments and Trends in Volcano Gravimetry. In: Nemeth K. (Ed.): *Updates in Volcanology: From Volcano Modelling to Volcano Geology*, doi: 10.5772/63420.
- Williams-Jones G., Rymer H., Mauri G., Gottsmann J., Poland M., Carbone D., 2008: Towards continuous 4D microgravity monitoring of volcanoes. *Geophysics*, **73**, 6, WA19–WA28, doi: 10.1190/1.2981185.
- Yokoyama I., Bonasia V., 1978: Gravity anomalies on the Thera Islands. In: Doulmas C. (Ed.): *Thera and the Aegean World I*. The Thera Foundation, London, 147–150.
- Yu H., Guo J., Kong Q., Chen X., 2019: Gravity Tides Extracted from Relative Gravimeter Data by Combining Empirical Mode Decomposition and Independent Component Analysis. In: Braitenberg C., Rossi G., *Geodynamics and Earth Tides* Editor group (Eds.): *Geodynamics and Earth Tides Observations from Global to Micro Scale*. Pageoph Topical Volumes. Birkhäuser, Cham, pp. 89–103, doi: 10.1007/978-3-319-96277-1\_9.

## Appendix 1

### *Gravity campaign of 1976*

Station	latitude	longitude	elevation	Gpotsdam	SDV	G(WGS84)	FAA
units	degrees	degrees	meter	mGal	mGal	mGal	mGal
2	36.3868	25.4308	1.596	979993.359	0.012	979979.349	127.32
3	36.3712	25.4823	5	979997.488	0.016	979983.477	133.843
4	36.3493	25.4	1	979971.133	0.016	979957.123	108.151
5	36.3496	25.4036	30	979966.828	0.016	979952.815	112.764
6	36.3596	25.4038	72.57	979953.732	0.018	979939.714	111.94
7	36.3666	25.4269	139.1	979953.863	0.019	979939.839	131.985
8	36.3571	25.4447	76.548	979979.705	0.028	979965.688	139.353
9	36.3564	25.4754	3.86	979997.139	0.019	979983.129	134.421
10	36.3437	25.4519	12.83	979988.615	0.017	979974.603	129.766
11	36.3863	25.4634	64.35	979981.414	0.015	979967.397	134.778
12	36.4006	25.4577	103	979969.792	0.017	979955.772	133.845
13	36.4226	25.4344	179.35	979943.187	0.017	979929.159	128.891
14	36.403	25.4373	190.18	979940.756	0.017	979926.727	131.5
15	36.4092	25.4798	18.34	979992.777	0.015	979978.766	129.971
16	36.4336	25.4273	296.45	979918.951	0.023	979904.912	139.832
17	36.4572	25.4211	228.79	979932.442	0.029	979918.41	130.415
18	36.4662	25.4028	185.99	979941.135	0.032	979927.106	125.122

19	36.4631	25.3828	121.8	979956.72	0.034	979942.698	121.177
20	36.4583	25.371	0.5	979985.647	0.034	979971.637	113.098
21	36.3688	25.4633	555.37	979865.998	0.034	979851.934	172.358
22	36.375	25.4531	328.28	979926.256	0.032	979912.214	162.02
23	36.3842	25.4465	303.96	979929.413	0.029	979915.374	156.881
24	36.3826	25.4336	258	979934.813	0.023	979920.777	148.237
25	36.4183	25.4277	0.7	979987.261	0.021	979973.251	118.225
26	36.411	25.4003	1.465	979981.058	0.023	979967.048	112.892
27	36.4045	25.3949	126.737	979952.283	0.024	979938.261	123.326
28	36.4075	25.3974	73.5	979963.959	0.017	979949.941	118.315
29	36.4118	25.3885	0	979978.203	0.016	979964.193	109.515
30	36.399	25.3805	1.021	979982.381	0.023	979968.371	115.108
31	36.4004	25.4049	2.962	979980.852	0.021	979966.841	114.06
32	36.3393	25.4324	9.24	979988.364	0.018	979974.353	128.786
33	36.4346	25.4362	123.537	979959.559	0.019	979945.537	127.011
34	36.4275	25.4599	3.27	979987.568	0.018	979973.558	118.527
35	36.4101	25.4462	137.21	979956.683	0.017	979942.659	130.472
36	36.3835	25.4787	26.85	979990.534	0.019	979976.521	132.569
37	36.3661	25.3659	1.3	979976.851	0.054	979962.841	112.509
38	36.3825	25.3497	0.1	979977.907	0.067	979963.897	111.775
39	36.4089	25.3526	2	979987.467	0.071	979973.456	119.644
40	36.4386	25.3513	1	979991.052	0.067	979977.041	120.353
41	36.4338	25.3443	160	979950.488	0.054	979936.462	129.255
mean	36.3982	25.4201	96.194	979965.341	0.026	979951.321	127.5
max	36.4662	25.4823	555.37	979997.488	0.071	979983.477	172.358
min	36.3393	25.3443	0	979865.998	0.012	979851.934	108.151
SDV	0.0342	0.0387	123.171	27.249	0.015	27.26	14.214

## Appendix 2

### *Gravity campaign of 2012*

Station	latitude	longitude	elevation	Gpotsdam	SDV	G(WGS84)	FAA
units	degrees	degrees	meter	mGal	mGal	mGal	mGal
1001	36.4031	25.4727	52.1	979987.902	0.011	979973.887	136.032
1002	36.4328	25.4224	360.07	979898.859	0.012	979884.814	139.44
1003	36.4619	25.3832	137.3	979952.422	0.012	979938.398	121.765
1004	36.458	25.3399	16.5	979979.231	0.035	979965.219	111.639
1005	36.442	25.3534	226.684	979930.486	0.037	979916.453	129.118
1006	36.4266	25.3467	294.979	979914.782	0.035	979900.743	135.815
1007	36.4128	25.3507	196.278	979935.385	0.034	979921.356	127.161
1008	36.43	25.3249	16.8	979987.517	0.029	979973.505	122.436
1009	36.4529	25.4237	316.775	979908.113	0.013	979894.072	133.603

1010	36.4608	25.3899	156.3	979947.616	0.014	979933.591	122.911
1011	36.4804	25.3824	7.9	979982.332	0.029	979968.321	110.15
1012	36.4728	25.4213	47.43	979974.742	0.017	979960.727	115.415
1013	36.4684	25.4242	6.53	979984.834	0.016	979970.824	113.266
1014	36.4634	25.4057	330.516	979901.835	0.015	979887.792	130.65
1015	36.4447	25.4436	59.508	979974.488	0.014	979960.472	121.314
1016	36.4338	25.448	77.183	979971.232	0.013	979957.214	124.452
1017	36.4045	25.3949	126.737	979952.669	0.013	979938.646	123.711
1018	36.4063	25.3965	100.2	979958.062	0.013	979944.042	120.759
1019	36.4084	25.3999	53.3	979970.412	0.014	979956.397	118.457
1020	36.4085	25.4013	57.399	979968.914	0.014	979954.898	118.217
1021	36.4102	25.3998	17.05	979977.126	0.014	979963.114	113.834
1022	36.4004	25.4049	2.962	979981.142	0.014	979967.132	114.35
1023	36.4042	25.4307	239.09	979925.667	0.014	979911.633	131.396
1024	36.3874	25.4367	300.28	979924.446	0.014	979910.407	150.497
1025	36.4136	25.4543	90.4	979969.938	0.014	979955.919	128.984
1026	36.4199	25.471	19.8	979987.618	0.012	979973.606	124.333
1027	36.4072	25.479	52.613	979986.584	0.013	979972.568	134.52
1028	36.3916	25.4862	2.9	979991.431	0.013	979977.42	125.382
1029	36.3836	25.4722	48.5	979985.844	0.013	979971.83	134.552
1030	36.3812	25.4491	307.4	979930.227	0.013	979916.187	159.013
1031	36.3688	25.4631	552.4	979866.396	0.014	979852.333	171.834
1032	36.3704	25.4584	500.1	979880.593	0.031	979866.535	169.76
1033	36.3862	25.4381	299.101	979928.231	0.012	979914.191	154.027
1034	36.3827	25.4336	259.969	979934.026	0.012	979919.99	148.047
1035	36.3826	25.3497	0.4	979978.069	0.013	979964.059	112.021
1036	36.3823	25.3475	2.3	979978.411	0.013	979964.401	112.976
1037	36.3822	25.3471	1.2	979978.216	0.013	979964.206	112.455
1038	36.3825	25.349	3.2	979977.847	0.013	979963.836	112.671
1039	36.3825	25.3497	0.1	979977.926	0.013	979963.916	111.795
1040	36.3939	25.3855	4.055	979981.558	0.014	979967.548	115.669
1041	36.3991	25.3804	2.529	979982.204	0.014	979968.194	115.393
1042	36.399	25.3805	1.021	979982.628	0.014	979968.618	115.355
1043	36.3969	25.3765	1.135	979980.803	0.013	979966.793	113.747
1044	36.3324	25.4424	1.72	979987.804	0.013	979973.793	126.497
1045	36.3566	25.4744	4.4	979997.352	0.013	979983.341	134.789
1046	36.3471	25.4386	169.52	979953.511	0.014	979939.485	142.705
1047	36.3576	25.3571	99.36	979950.637	0.014	979936.617	117.277
1048	36.357	25.3592	134.822	979940.836	0.014	979926.813	118.469
1049	36.3588	25.3892	210.06	979923.049	0.013	979909.019	123.735
1050	36.3526	25.3996	91.8	979949.822	0.013	979935.803	114.564
1051	36.3754	25.4256	198.99	979941.401	0.012	979927.371	137.24
1052	36.3653	25.4769	365.574	979912.002	0.013	979897.956	160.107
2000	36.4073	25.4786	34.61	979992.925	0.009	979978.912	135.305

mean	36.4036	25.4096	125.658	979956.945	0.016	979942.923	127.728
max	36.4804	25.4862	552.4	979997.352	0.037	979983.341	171.834
min	36.3324	25.3249	0.1	979866.396	0.009	979852.333	110.15
SDV	0.0355	0.0451	140.185	31.721	0.007	31.734	15.264

## Appendix 3

### *Gravity campaign of 2014*

Station	latitude	longitude	elevation	Gpotsdam	SDV	G(WGS84)	FAA
units	degrees	degrees	meter	mGal	mGal	mGal	mGal
1001	36.4031	25.4727	52.1	979987.896	0.013	979973.881	136.026
1017	36.4045	25.3949	126.737	979952.693	0.015	979938.67	123.735
1020	36.4085	25.4013	57.399	979968.923	0.027	979954.907	118.226
1033	36.3862	25.4381	299.101	979928.238	0.015	979914.199	154.035
1034	36.3827	25.4336	259.969	979934.009	0.014	979919.974	148.031
1047	36.3576	25.3571	99.269	979950.664	0.013	979936.644	117.276
1100	36.3868	25.4308	1.596	979993.43	0.009	979979.42	127.392
1101	36.3751	25.48	22.701	979994.1	0.013	979980.087	135.584
1102	36.4119	25.4373	181.272	979945.138	0.016	979931.111	132.366
1103	36.4201	25.4306	237.125	979929.31	0.017	979915.277	133.056
1104	36.4183	25.4277	1.14	979987.004	0.019	979972.994	118.104
1105	36.4104	25.4012	2.01	979981.549	0.022	979967.539	113.597
1106	36.4092	25.4009	59.357	979968.223	0.023	979954.207	118.07
1107	36.4075	25.3979	72.146	979964.612	0.023	979950.595	118.551
1108	36.4053	25.3958	120.925	979953.385	0.026	979939.363	122.564
1109	36.4042	25.3966	120.958	979953.887	0.026	979939.866	123.167
1110	36.4056	25.3956	124.87	979951.893	0.027	979937.87	122.262
1111	36.411	25.4003	1.465	979981.315	0.026	979967.305	113.149
1112	36.4104	25.4015	2.471	979981.843	0.027	979967.833	114.038
1113	36.3556	25.446	68.104	979980.36	0.016	979966.343	137.533
1114	36.4599	25.4167	189.085	979942.344	0.017	979928.315	127.83
1115	36.4603	25.4165	192.386	979941.121	0.019	979927.092	127.589
1116	36.4619	25.4142	180.935	979944.352	0.019	979930.324	127.154
1117	36.4627	25.4131	218.668	979934.477	0.019	979920.445	128.848
1118	36.4613	25.416	185.52	979944.13	0.017	979930.102	128.396
1119	36.4665	25.3684	3.837	979983.961	0.018	979969.951	111.731
1120	36.4624	25.3697	26.698	979978.365	0.019	979964.352	113.541
1121	36.4752	25.3828	30.285	979978.569	0.021	979964.556	113.746
1122	36.4768	25.4076	15.726	979982.373	0.021	979968.361	112.917
1123	36.4652	25.4211	37.457	979979.747	0.021	979965.734	117.997
1124	36.4631	25.4243	33.074	979979.999	0.021	979965.986	117.085
1125	36.4609	25.4208	122.078	979959.431	0.019	979945.409	124.164

1126	36.4574	25.4195	214.354	979936.5	0.018	979922.469	130
1127	36.4099	25.4417	168.536	979949.093	0.015	979935.066	132.564
1128	36.3577	25.3561	78.012	979956.322	0.016	979942.304	116.367
1129	36.3578	25.3553	54.4	979962.648	0.018	979948.632	115.405
1130	36.3634	25.3855	158.838	979935.521	0.02	979921.496	120.01
1131	36.3481	25.3876	2.842	979972.228	0.02	979958.218	109.914
1132	36.3561	25.3817	121.471	979945.759	0.02	979931.737	119.349
1133	36.3545	25.3761	4.195	979973.971	0.02	979959.961	111.524
1134	36.3638	25.364	51.775	979963.809	0.018	979949.794	115.239
1135	36.3581	25.3666	96.039	979953.643	0.016	979939.623	119.218
1136	36.3372	25.4334	1.615	979990.62	0.015	979976.61	128.864
1137	36.246	25.2094	9.684	979994.209	0.016	979980.198	142.814
1138	36.2463	25.2092	28.758	979988.054	0.019	979974.041	142.513
1139	36.2469	25.2084	34.67	979987.049	0.02	979973.035	143.286
1140	36.2476	25.2083	44.553	979983.864	0.021	979969.85	143.083
1141	36.2502	25.2076	50.131	979981.802	0.022	979967.787	142.518
1142	36.251	25.2073	41.312	979983.324	0.021	979969.31	141.255
1143	36.2454	25.2072	53.158	979980.966	0.02	979966.951	143.03
1144	36.2446	25.2077	46.007	979982.301	0.019	979968.286	142.229
1145	36.3835	25.4394	290.706	979931.228	0.015	979917.189	154.669
1146	36.3801	25.4816	16.459	979994.036	0.016	979980.024	133.164
1147	36.3874	25.4633	77.755	979983.622	0.016	979969.604	141.026
1148	36.4007	25.4573	105.262	979969.393	0.018	979955.373	134.135
1149	36.4015	25.4489	147.973	979956.833	0.02	979942.809	134.682
1150	36.3935	25.4499	171.718	979957.03	0.021	979943.003	142.897
1151	36.4098	25.4532	106.424	979966.491	0.022	979952.47	130.809
1152	36.414	25.4445	135.254	979957.597	0.022	979943.574	130.441
1153	36.4159	25.4365	180.771	979945.292	0.022	979931.265	132.02
1154	36.4228	25.4392	150.228	979953.264	0.022	979939.24	129.973
1155	36.4289	25.4586	18.216	979985.482	0.021	979971.47	120.937
1156	36.4346	25.4362	123.537	979959.566	0.02	979945.544	127.019
1157	36.4344	25.429	272.552	979925.636	0.018	979911.599	139.075
1158	36.3851	25.4345	232.738	979946.111	0.016	979932.078	151.524
1159	36.3866	25.4279	2.725	979992.235	0.019	979978.225	126.562
1160	36.386	25.4284	2.311	979992.938	0.013	979978.928	127.192
1161	36.3884	25.4319	3.322	979993.606	0.012	979979.596	127.961
1162	36.3596	25.4023	72.819	979954.575	0.017	979940.558	112.855
1163	36.3618	25.3877	174.667	979932.724	0.025	979918.697	122.238
1165	36.3592	25.4013	76.279	979953.423	0.025	979939.406	112.808
1166	36.3596	25.4008	78.295	979952.647	0.031	979938.63	112.615
1167	36.3598	25.4094	83.007	979954.214	0.024	979940.196	115.62
1168	36.3638	25.4249	119.301	979957.26	0.027	979943.238	129.515
1169	36.3452	25.4249	7.194	979981.962	0.024	979967.951	121.239
1170	36.3481	25.4267	40.771	979975.161	0.029	979961.147	124.545

1171	36.3577	25.4295	108.139	979962.054	0.023	979948.033	131.394
1172	36.3388	25.4438	6.1	979989.79	0.021	979975.779	129.281
1173	36.3407	25.4558	3.46	979990.533	0.025	979976.522	129.047
1174	36.3539	25.4734	3.896	979996.732	0.026	979982.722	134.246
1175	36.3571	25.4447	76.548	979979.692	0.026	979965.674	139.339
1176	36.3666	25.4269	138.882	979954.117	0.024	979940.093	132.171
1178	36.3607	25.4041	13.078	979968.997	0.023	979954.985	108.751
1179	36.361	25.4052	22.924	979966.522	0.03	979952.51	109.293
1180	36.3871	25.431	4.287	979993.457	0.025	979979.446	128.224
1181	36.4084	25.4	52.67	979970.592	0.026	979956.577	118.446
1182	36.4607	25.39	155.73	979947.675	0.015	979933.65	122.806
1183	36.4063	25.3967	100.58	979957.942	0.024	979943.922	120.754
1184	36.3874	25.4367	300.11	979924.501	0.013	979910.462	150.503
2000	36.4073	25.4786	34.679	979992.918	0.005	979978.904	135.319
mean	36.3844	25.4	90.202	979965.854	0.02	979951.835	127.356
max	36.4768	25.4816	300.11	979996.732	0.031	979982.722	154.669
min	36.2446	25.2072	1.14	979924.501	0.009	979910.462	108.751
SDV	0.057	0.0665	80.895	19.885	0.004	19.892	11.267